Published in final edited form as:
J Invest Dermatol. 2008 January ; 128(1): 162–174.

Involvement of Dynein and Spectrin with Early Melanosome Transport and Melanosomal Protein Trafficking

Hidenori Watabe[1,2,*], **Julio C. Valencia**[1,*], **Elodie Le Pape**[1], **Yuji Yamaguchi**[1], **Masayuki Nakamura**[2], **François Rouzaud**[1], **Toshihiko Hoashi**[1], **Yoko Kawa**[2], **Masako Mizoguchi**[2], and **Vincent J. Hearing**[1]

1*Laboratory of Cell Biology, National Cancer Institute, National Institutes of Health, Bethesda, MD, USA*

2 *Department of Dermatology, St. Marianna University School of Medicine, Kawasaki, Japan*

Abstract

Melanosomes are unique membrane-bound organelles specialized for the synthesis and distribution of melanin. Mechanisms involved in the trafficking of proteins to melanosomes and in the transport of mature pigmented melanosomes to the dendrites of melanocytic cells are being characterized but details about those processes during early stages of melanosome maturation are not well understood. Early melanosomes must remain in the perinuclear area until critical components are assembled. In this study, we characterized the processing of two distinct melanosomal proteins, TYR and Pmel17, to elucidate protein processing in early or late steps of the secretory pathway, respectively, and to determine mechanisms underlying the subcellular localization and transport of early melanosomes. We used immunological, biochemical and molecular approaches to demonstrate that the movement of early melanosomes in the perinuclear area depends primarily on microtubules but not on actin filaments. In contrast, the trafficking of TYR and Pmel17 depends on cytoplasmic dynein and its interaction with the spectrin/ankyrin system which is involved with the sorting of cargo from the plasma membrane. These results provide important clues towards understanding the processes involved with early events in melanosome formation and transport.

Keywords

tyrosinase; Pmel17; processing; trafficking; pigmentation; melanosome

INTRODUCTION

Melanosomes are unique membrane-bound organelles that are specialized for the synthesis and the distribution of melanin (Hearing, 2000; Kushimoto et al., 2001; Kushimoto et al., 2003). Melanosomes are produced only by melanocytic cells and normally mature from undifferentiated and unpigmented organelles (termed stage I melanosomes) to differentiated and highly pigmented organelles (termed stage IV melanosomes). Melanosomes are often divided into “early” (i.e. stages I and II) or “late” (i.e. stages III and IV) melanosomes which lack or contain pigment, respectively. Tyrosinase (TYR) is an enzymatic protein localized in melanosomes that catalyzes the critical rate-limiting step required for melanin synthesis, i.e. tyrosine hydroxylation (Körner and Pawelek, 1982; Ujvari et al., 2001; Francis et al., 2003; Hearing and Ekel, 1976). The trafficking of TYR to melanosomes can be affected dramatically by mutations in several melanogenic genes and by changes of intracellular pH that result in

Address correspondence to: Vincent J. Hearing, Laboratory of Cell Biology, Building 37, Room 2132, National Institutes of Health, Bethesda, MD 20892, USA.; Tel: 301-496-1564; FAX: 301-402-8787; E-mail: hearingv@nih.gov.
*H. Watabe and J.C. Valencia contributed equally to this study.

oculocutaneous albinism or hypopigmentation, respectively (Oetting et al., 2003; Halaban et al., 1997; Halaban et al., 2002; Watabe et al., 2004). Pmel17 (also known as gp100) is a structural protein of melanosomes that is critical to forming the internal fibrillar matrix characteristic of stage II melanosomes (Kushimoto et al., 2001). The trafficking of Pmel17 to melanosomes is rarely disrupted since it sorts through both the endocytic and the secretory pathways with relatively high efficiency (Valencia et al., 2006; Valencia et al., 2007). Those characteristics make these two melanosomal proteins suitable targets to study distinct routes of protein trafficking to melanosomes and the transport of those organelles from perinuclear areas of melanocytes to their periphery prior to their transfer to neighboring keratinocytes.

In melanocytes, mature pigmented melanosomes bind to microtubules and undergo actin-dependent transport towards the cell periphery prior to their transfer to keratinocytes (Wu et al., 2002). Thus, the intracellular transport of melanosomes is directed by microtubules (composed of α:β-tubulin dimers) and actin filaments (composed of actin monomers). Microtubules serve as tracks for the transport of several intracellular organelles, including lysosomes and sorting vesicles (Lambert et al., 1999; Robertson and Allan, 2000). The trafficking of sorting vesicles to their target organelles is controlled by two classes of microtubule-associated motor proteins, kinesins and cytoplasmic dyneins. Kinesins power the plus end directed microtubule-based motility, while cytoplasmic dyneins drive the minus end motility (Vallee et al., 1988; Schnapp and Reese, 1989). Dyneins and kinesins also have well established roles in retrograde and in anterograde transport of melanosomes (Wu and Hammer, III, 2000; Vancoillie et al., 2000a; Hara et al., 2000; Byers et al., 2000). A recent study of melanocytic cells in the amphibian *Xenopus laevis* suggested that the distribution of melanosomes in those cells results from competition between the microtubule-based dyneins and the actin-based myosins, in what was termed a “continual tug-of-war” (Gross et al., 2002). In their model, myosin-Va counteracts dynein-mediated motor transport more effectively than kinesin- mediated transport which results in the eventual localization of mature melanosomes at the periphery of the cells. Recently, there has been confirmation that a similar mechanism is responsible for melanosome transport in retinal pigment epithelial cells (Lopes et al., 2007). Thus, mechanisms underlying the movement of mature pigmented melanosomes are fairly well characterized, but during their early formative stages, melanosomes need to remain in the perinuclear area until important enzymatic and structural components are delivered. In addition to pigmented MNT1 melanoma cells, we have used SK-Mel-28 melanoma cells, which express all known melanosomal proteins yet remain unpigmented and produce only early stage melanosomes, to characterize events important to the subcellular localization of those organelles. Interestingly, microtubules are essential both for dispersion and for aggregation of melanosomes in zebrafish after stimulation with α-melanocyte stimulating hormone (αMSH), while microfilaments affect only their aggregation (Logan et al., 2006). However, whether αMSH or its antagonist, agouti-signaling protein (ASP), regulates the expression of motor proteins in mammalian melanocytes is unknown.

Spectrin is a cytoskeletal protein that binds simultaneously to integral membrane proteins, cytosolic proteins and certain phospholipids (either directly or through adaptor proteins) to create a multifunctional scaffold. Spectrin also binds to all major filament systems and links membranes and cytosolic proteins to cytoskeletal elements (reviewed in (De Matteis and Morrow, 2000)). Current evidence indicates that the spectrin skeleton plays a role in the early secretory pathway at the endoplasmic reticulum (ER)-Golgi interface (Godi et al., 1998). Nevertheless, there is limited evidence for a role of spectrin in post-Golgi trafficking and in the control of endo\lysosomal compartments (Michaely et al., 1999; De Matteis and Morrow, 2000). A recent study revealed that spectrin localizes in melanophores and plays a role in the transport of melanosomes within melanocytic cells of amphibians (Aspengren and Wallin, 2004), but to date nothing is known about the possible role of the spectrin skeleton in mammalian melanocytes.

SK-Mel-28 melanoma cells are unpigmented due to a disrupted endocytic pathway that severely affects the endosomal trafficking of TYR, but not the trafficking of Pmel17, since those cells form stage II melanosomes which depend on Pmel17 function (Watabe et al., 2004). Therefore, we used SK-Mel-28 cells as a model to study mechanisms involved in the trafficking of melanosomal proteins and in the localization of early melanosomes. Analysis of the trafficking of TYR and Pmel17 demonstrated that early melanosomes are transported primarily along the microtubule network and may involve the microtubule-based motor dynein. Proteomic and immunofluorescence analysis revealed for the first time the presence of spectrin in early melanosomes of human melanocytes. Further, the primarily central localization of spectrin in melanocytic cells suggests its role in the aggregation rather than the dispersion of melanosomes. In this regard, spectrin may be involved in the linkage of sorting vesicles, which contain either TYR or Pmel17, to melanosomes. DNA μarray analysis showed that key elements involved in the transport of melanosomes, such as Rab27A and dynein, are strongly down-regulated by ASP, which suggests that melanosome transport is disrupted by ASP and further inhibits melanogenesis. Thus, this study provides important clues towards understanding the roles and the mechanisms involved in the maturation and transport of early melanosomes.

RESULTS and DISCUSSION

Motor-related proteins detected in melanosomes at various stages of maturation

Studies of the dynamics of mature melanosomes in pigmented melanocytic cells have been critical to unraveling the roles of important motor components in the intracellular transport of organelles. However, mechanisms involved in the transport of early melanosomes and their accumulation in perinuclear areas of melanocytic cells are unknown. Our recently published global proteomics analysis of melanosomes (Chi et al., 2006) permits a comparison of proteins present in early and/or late melanosomes derived from pigmented MNT-1 cells with those in early melanosomes derived from unpigmented SK-Mel-28 cells. Motor-related proteins found in early and/or late melanosomes are summarized in Table 1. From the tripartite complex of Rab27A, melanophilin (SLAC2A) and myosin-Va, which connects mature melanosomes to the actin cytoskeleton (Wu et al., 2006), only Rab27A was present in early melanosomes from both types of melanocytic cells. Interestingly, myosin-Va was present only in melanosomes from pigmented MNT-1 cells, while melanophilin was not detected in melanosomes from either type of cell.

Similarly, we searched for the microtubule-based motor proteins kinesin and cytoplasmic dynein, which bind the actin-based motor protein myosin-Va for anterograde melanosome transport (Byers et al., 2000; Vancoillie et al., 2000b; Vancoillie et al., 2000a). Kinesin was found only in melanosomes from pigmented MNT-1 cells, while dynein light chain proteins were found in melanosomes from both types of melanocytic cells. These results suggest that early melanosomes are transported via a balanced coordination between kinesins and dyneins in melanocytic cells. However, dynein-dependent motor transport may be predominant in early melanosomes from unpigmented SK-Mel-28 cells, which is consistent with their accumulation in the perinuclear area. Recently it has been reported that the dynactin complex binds both dynein and kinesin 2 and is required for plus-end-directed melanosome transport in amphibian melanophores (Deacon et al., 2003). In our study, dynactin 1 ($p150^{glued}$) and dynamitin (p50), key elements of the dynactin complex, were detected only in mature (stage IV) melanosomes. These results are consistent with the dual role of this complex in mediating two-way organelle traffic.

The spectrin/ankyrin skeleton is thought to bridge integral membrane proteins, cytosolic proteins and certain phospholipids to form a versatile adaptor scaffold. Several studies support a growing body of evidence that beyond the Golgi, many if not all other compartments of the

secretory and endo/lysosomal pathways have associated skeletons (reviewed in (De Matteis and Morrow, 2000)). Spectrin has been identified in several lysosomal-related organelles such as chromaffin granules and synaptic vesicles (Zagon et al., 1986; Aunis and Bader, 1988), and more recently, it has been found in melanosomes in amphibians (Aspengren and Wallin, 2004). Our proteomics analysis identified spectrin-α and spectrin-β II in melanosomes from both types of human melanocytic cells (Table 1). Note that spectrin-β IV, which is associated with secretory granules, was only detected in early stage melanosomes from SK-Mel-28 cells. Interestingly, the adaptor protein ankyrin, which provides the primary linkage between the spectrin-actin network and the plasma membrane, was not detected in any melanosome fractions. However, the cytoplasmic protein myotropin (V1), which contains three ankyrin repeats and is involved in the regulation of actin polymerization (Taoka et al., 2003), was identified in early melanosomes from SK-Mel-28 cells. Interestingly, two α-actinins were detected only in early stage melanosomes from unpigmented SK-Mel-28 cells. α-Actinins belong to the spectrin gene superfamily which represents a diverse group of cytoskeletal proteins that includes the α- and β-spectrins and dystrophins. α-Actinin is an actin-binding protein with multiple roles in different types of cells. In nonmuscle cells, the cytoskeletal isoform of α-actinin is found along microfilament bundles and adherens-type junctions, where it is involved in binding actin to the membrane (Broderick and Winder, 2005). This result further supports an important role for the spectrin skeleton in early melanosomes. The sum of these results suggests that dynein and spectrin are present in early melanosomes and thus may be involved in their subcellular localization in melanocytic cells along with the Rab27/ melanophilin/ myosin-Va motor and the dynactin complex which is involved in the transport of mature pigmented melanosomes.

Unpigmented melanocytic cells have an altered distribution of kinesin and spectrin

We then compared the distribution of various motor-related proteins (Fig. 1), including β-tubulin (as a marker for microtubules), kinesins, dyneins and spectrin, with the localization of TYR and Pmel17 in pigmented MNT-1 cells (left panels in each set) and in unpigmented SK-Mel-28 cells (right panels in each set). In MNT-1 cells, TYR and Pmel17 were evenly distributed throughout the cytoplasm. In contrast, in SK-Mel-28 cells, those proteins showed a predominant perinuclear pattern in all cells, while in ~15% of SK-Mel-28 cells, a diffuse and less prominent cytoplasmic pattern was evident. TYR or Pmel17 colocalized with organized fibers of microtubules beneath the plasma membrane and especially in dendrites of MNT-1 cells (Fig. 1A). However, in SK-Mel-28 cells, the microtubule network was concentrated near the perinuclear area with thin fibers extending to the periphery in a disrupted pattern. In SK-Mel-28 cells, β-tubulin colocalized with TYR and Pmel17 mainly in the perinuclear area (inset) but not in the dendrites. Next, we compared the distribution of kinesin and dynein with TYR and Pmel17. Kinesin (Fig. 1B) showed a well defined distribution in the peripheral cytoplasm and in the dendrites but not in the perinuclear area in pigmented or in unpigmented melanocytic cells. A limited colocalization between kinesin and TYR or Pmel17 was observed at the dendrite tips (insets) in both types of cells. In contrast, dynein (Fig. 1C) showed a diffuse granular pattern that colocalized with granules containing either TYR or Pmel17 near the perinuclear area (insets) in both types of melanocytic cells. These results suggest that dynein-dependent motor transport is predominant in early melanosomes, while mature late stage melanosomes are transported actively to the dendrites by kinesin. This is consistent with the absence of kinesin in early melanosomes from SK-Mel-28 cells.

Analysis of the spectrin distribution also revealed differences between MNT-1 cells and SK-Mel-28 cells (Fig. 1D). Spectrin showed a well-defined distribution at the plasma membrane in the central areas of MNT-1 cells but not in their dendrites. Note that the staining of spectrin at the plasma membrane was enhanced at points of cell-cell contact. Surprisingly, there was no staining of spectrin at the plasma membrane of SK-Mel-28 cells. In both types of cells,

spectrin in the cytoplasm was distributed mainly in the perinuclear area where it colocalized with granules containing either TYR or Pmel17, but was not detected in the dendrites of the cells. Taken together, these results show dramatic differences in the distribution of kinesin and spectrin that may be involved in the perinuclear localization of early melanosomes in unpigmented SK-Mel-28 cells. Further, the presence of spectrin in perinuclear areas but not in the dendrites, and its relationship with early melanosomes, suggests a role for spectrin in the aggregation rather than in the dispersion of melanosomes in mammalian melanocytes.

Monitoring of early and late trafficking of melanosomal proteins in the secretory pathway

Protein and vesicle trafficking in the secretory pathway can be separated into early events (for trafficking within the ER-Golgi) and late events (for trafficking from the TGN to target organelles). To evaluate these processing events independently, we characterized the trafficking of TYR and Pmel17 in SK-Mel-28 cells. First, we compared the processing of TYR and Pmel17 using metabolic pulse-chase labeling (Fig. 2A). In MNT-1 cells (left panel), αPEP7h recognized TYR as a ~72 kDa band at 0 hr of chase that was slowly glycosylated to ~78 kDa after 6 hr of chase; the intensity of that band was reduced by 53% after 48 hr of chase. Similarly, αPEP13h recognized Pmel17 in MNT-1 cells as a single ~95 kDa band at 0 min of chase, then as a ~115 kDa band which appeared after 15 min of chase. Note that the intensity of Pmel17 was reduced by 47% after 3 hr of chase. In contrast, in SK-Mel-28 cells (right panel), TYR and Pmel17 seemed to be processed correctly at early chase times but their stability was severely reduced when compared with MNT-1 cells, by 83% and 90%, respectively.

Next, we used electron microscopy to determine the localization of TYR in MNT-1 cells and in SK-Mel-28 cells (Fig. 3). Cells were stained with or without L-3,4-dihydroxyphenylalanine (DOPA), which is converted into electron dense DOPA-melanin by TYR, allowing the distribution of DOPA melanin to be assessed. In MNT-1 cells, melanosomes from different stages of maturation, especially pigmented ones, are distributed randomly throughout the cytoplasm (Fig. 3A). DOPA staining was mainly observed in stage II and stage III melanosomes (Fig. 3B). In some cases, Golgi structures showed intense DOPA staining (Fig. 3C, arrowheads). In unstained SK-Mel-28 cells (Fig. 3D), stage II melanosomes were observed scattered throughout the cytoplasm and near the plasma membrane, which is evidence that Pmel17 was processed correctly. Interestingly, DOPA staining (Fig. 3E) revealed a fine granular staining pattern inside several organelles, such as multivesicular bodies (MVB; asterisks). Note the fine granular DOPA staining (Fig. 3F) in vesicular organelles (open arrowheads) and very few stage II melanosomes (dark arrowheads). Note that the DOPA melanin pattern inside vesicular organelles has a diffuse and less organized pattern compared with stage II melanosomes (Fig. 3F, inset). This result indicates that the small amount of TYR sorted from the TGN in unpigmented SK-Mel-28 cells is mostly misdirected to MVB rather than being sorted to melanosomes, which probably results in its rapid degradation. In contrast, Pmel17 is sorted and incorporated correctly into early melanosomes in SK-Mel-28 cells.

Taken together, we conclude that because of its longer processing time in the ER-Golgi compartment, TYR is a good target to study melanosome protein trafficking in the early secretory pathway. In contrast, the rapid and uninterrupted trafficking of Pmel17 makes it a suitable marker to analyze vesicle sorting and early melanosome transport at late stages of the secretory pathway.

Microtubules are responsible for anterograde trafficking in the early secretory pathway

Bidirectional traffic from the ER-Golgi intermediate compartment (ERGIC) to the ER and Golgi depends on intact microtubules (Ben-Tekaya et al., 2005). Because it is the ERGIC to *cis*-Golgi step that requires intact microtubules, we tested the processing and trafficking of TYR and Pmel17 in cells treated with or without nocodazole, an agent that disrupts microtubule

function and disrupts the Golgi complex (Salas et al., 1986). SK-Mel-28 cells were metabolically pulse-labeled and were then incubated with nocodazole and chased for various times. TYR and Pmel17 were immunoprecipitated with αPEP7h and αPEP13h antibodies, respectively (Fig. 4A). In nocodazole-treated SK-Mel-28 cells, TYR and Pmel17 seemed to be processed normally, but a much weaker mPmel17 band (open arrow) was noted compared to untreated cells (compare with Fig. 2A). We then examined the sensitivity of TYR to EndoH, an enzyme which removes high-mannose and hybrid type carbohydrates (Toyofuku et al., 2001; Costin et al., 2003), to evaluate whether nocodazole affected TYR processing through the Golgi (Fig. 4B). TYR was only partially sensitive to EndoH after 3 hr of chase and that was associated with a slight increase in stability after 24 hr of chase in untreated SK-Mel-28 cells. In contrast, TYR was completely sensitive to EndoH at all chase times in nocodazole-treated cells. To further confirm those results, lysates of SK-Mel-28 cells treated or untreated with nocodazole were digested with or without EndoH and were analyzed by immunoblotting (Fig. 4C). In untreated SK-Mel-28 cells, TYR had EndoH-sensitive (S) and resistant (R) bands as expected, but in nocodazole-treated SK-Mel-28 cells, TYR was again fully sensitive to EndoH digestion. These results suggest that nocodazole alters anterograde trafficking of TYR because it affects its maturation in the Golgi.

Since pH neutralizing agents, such as bafilomycin, improve the sorting of TYR in SK-Mel-28 cells (Watabe et al., 2004), we evaluated whether TYR can be rescued by combined treatment with nocodazole and bafilomycin (Fig. 4C, right panel). TYR remained EndoH-sensitive despite the presence of a weak EndoH-resistant band. The sum of these results suggests that the anterograde transport and processing of TYR in the ER-Golgi compartment depends on microtubules. The effect on protein processing is probably due to arrested movement through the Golgi, preventing access to glycosylation enzymes, as reported previously (Presley et al., 1997).

Actin filaments are critical for sorting in the early secretory pathway

To further evaluate the role of actin filaments in melanosome transport, we characterized the intracellular distribution of F-actin in MNT-1 cells and in SK-Mel-28 cells (Fig. 5A). Dual immunofluorescence revealed that actin filaments were distributed mainly at the cell periphery with fibers observed across the pigmented MNT-1 cells (arrow). In contrast, two distinct patterns of actin filaments were observed in unpigmented SK-Mel-28 cells. One pattern showed actin fibers crossing the cell in several directions (arrows) while the other pattern showed a predominantly granular pattern in some areas (arrowheads). Colocalization of F-actin with TYR was scattered in both types of melanocytic cells near the perinuclear area and also in the dendrite tips of MNT-1 cells. Thus our results suggest that actin filaments may not be critical for TYR trafficking in the early secretory pathway.

Actin filaments are responsible for the intracellular localization of vATPases (Vitavska et al., 2003; Chen et al., 2004) and for maintaining the morphology of Golgi cisternae (Lazaro-Dieguez et al., 2006). We then evaluated whether treatment with cytochalasin D affected the sensitivity of TYR to EndoH digestion using immunoblotting analysis both in SK-Mel-28 cells and in MNT-1 cells (Fig. 5C). In cytochalasin D treated cells, TYR was either mostly sensitive (SK-Mel-28 cells) or mostly resistant (MNT-1 cells) to EndoH digestion despite the apparently unaltered size of the protein. Cytochalasin D is known to produce severe swelling of the Golgi cisternae, which leads to a completely disorganized structure and an increase of intra-Golgi pH (Lazaro-Dieguez et al., 2006). To rule out the possibility that previously formed TYR is affecting the appearance of EndoH-resistant bands, we treated cells for 3 hr with cytochalasin D and bafilomycin A1, an agent known to improve TYR stability and processing in the Golgi of melanoma cells (Watabe et al., 2004) (Fig. 5C, right). In SK-Mel-28 cells, TYR processing

was rescued producing a strong EndoH-resistant band. Consistently, a severe reduction in the intensity of the lower band sensitive to EndoH was observed in MNT-1 cells.

The sum of these results suggests that anterograde trafficking of melanosomal proteins, such as TYR, in the early secretory pathway depends both on pH and on microtubules. In contrast, actin filaments are mainly associated with maintaining Golgi morphology and in retrograde transport at this early stage of the secretory pathway (Valderrama et al., 2001).

TYR and Pmel17 are sorted directly to melanosomes in SK-Mel-28 cells

It is well known that TYR follows an indirect sorting pathway through endosomes to reach melanosomes (Watabe et al., 2004) while Pmel17 follows both direct and indirect pathways to get to those organelles (Valencia et al., 2006). Since the endocytic pathway is severely disrupted in SK-Mel-28 cells, we hypothesized that TYR and Pmel17 are sorted to melanosomes using a common pathway, probably one mediated by adaptor protein (AP) complexes. To test that hypothesis, we characterized the presence and distribution of AP complexes in SK-Mel-28 cells (Fig. 6). First, we isolated several subcellular compartments using a combination of sucrose and iodixonadol gradients and analyzed them by immunoblotting. In the plasma membrane, TYR and Pmel17 were detected in small quantities compared to total cell extracts (Fig. 6A). Furthermore, MART1, α-adaptin (AP2) and clathrin were detected in the plasma membrane as well. The enrichment of integrin 5α, a plasma membrane marker, supports the purity of that fraction.

Our proteomics analysis identified only the α- and μ- subunits of AP2 in early melanosomes from SK-Mel-28 cells (Chi et al., 2006). Immunoblot analysis of early melanosomes confirmed that AP2 had the strongest signal in those organelles, followed by very weak bands for AP1 and AP3 (Fig. 6B). Note the presence of AP1, AP2 and AP3 in endosomes and in clathrin coated vesicle (CCV) fractions, which were used as positive controls. Next, we evaluated the distribution of TYR and Pmel17 with AP1, AP2 and/or AP3 in SK-Mel-28 cells using dual immunofluorescence (Fig. 6C). TYR and Pmel17 were mainly localized in the perinuclear area, although both proteins were present in the dendrites of SK-Mel-28 cells as well. Colocalization of TYR and Pmel17 with AP1 and AP3 was strong in the perinuclear area, probably as a result of their accumulation in the ER-Golgi compartment. In contrast, Pmel17 showed a wider cytoplasmic colocalization with AP2 than with TYR inside granular structures. These results validate our proteomics study and suggest a major role for AP2 in the trafficking of melanosomal proteins to early melanosomes. Thus, from these results, we conclude that in unpigmented SK-Mel-28 cells, TYR and Pmel17 are sorted through the plasma membrane to early melanosomes in vesicles containing AP2.

Physiological regulation of motor protein expression

Since mature pigmented melanosomes are transported to the tips of dendrites in melanocytic cells, we hypothesized that hormones regulating pigmentation, such as αMSH and/or its physiological antagonist ASP, may regulate the expression of motor proteins and thus affect that process. We tested that hypothesis by evaluating the effects of αMSH and ASP on melan-a melanocytes, which have been previously used to characterize hormonal regulation of pigmentation (Furumura et al., 1996; Sakai et al., 1997; Abdel-Malek et al., 2001). We performed DNA μarray analysis of melanocytes treated for 3 days either with αMSH or with ASP. The results obtained regarding expression of motor-related proteins are summarized in Table 2.

From the complex of RAb27A, melanophilin and myosin-Va, DNA μarray analysis revealed that only Rab27A was down-regulated significantly by ASP. This is the first evidence that expression of Rab27 is regulated by pigmentary hormones. Surprisingly, dyneins and ARP1,

major components of the macromolecular complex of dynactin (Schnapp and Reese, 1989), were also significantly down-regulated by ASP while Dnai2 was up-regulated by MSH. Note that dyneins and Rab27A are present in early melanosomes from SK-Mel-28 cells by proteomic analysis (Table 2). No elements of the spectrin skeleton were regulated significantly either by αMSH or by ASP. The DNA μarray analysis also showed that several components of the microtubule anterograde transport machinery, including tubulin α4A (Tuba4a), tubulin-folding cofactor E (TBCE) and kinesin family members 21A and 21B, were down-regulated by ASP, except for kinesin family member 15 which was up-regulated by αMSH. In an attempt to validate the dramatic effects observed for ASP on melan-A cells, MNT-1 cells and SK-Mel-28 cells were treated with or without ASP for 3 days. Cell lysates were then prepared and levels of several motor proteins were analyzed by immunoblotting (Fig. 7). In SK-Mel-28 cells (Fig. 7A), ASP down-regulated expression of Rab27, dynein, and kinesin proteins. No change was observed for tubulin or spectrin. In contrast, in MNT-1 cells (Fig. 7B), ASP down-regulated the key motor protein dynein, while no change was observed in other motor proteins, including Rab 27. In both melanoma cell lines, TYR was down-regulated by ASP, although this was more evident in SK-Mel-28 cells. These results are consistent with the reduction in TYR activity previously reported for ASP (Furumura et al., 1996). The reason for the differences observed among melanoma cells is not clear. One could argue that the high pigmentation level of MNT-1 cells may have played a role in the reduced effect of ASP. However, to date there has been no report of the effects of ASP on human melanoma cells. In any case, ASP consistently reduced the RNA and protein levels of at least one key motor protein, dynein, as well as the key melanin producing enzyme, TYR.

Taken together, these results suggest that the expression of key motor proteins is physiologically regulated by αMSH and/or by ASP in melanocytic cells. αMSH promoted the expression of proteins related to the anterograde transport of melanosomes. These results also show, for the first time, that ASP disrupts both pigmentation and melanosome transport by down-regulating key motor proteins such as dynein.

Final Considerations

Genetic and biochemical studies have identified several coat-color mutations in mice that affect the transport of melanosomes (i.e. *ashen, leaden and dilute*) (Wu and Hammer, III, 2000). All 3 of those genes affect actin-based rather than microtubule-based melanosome motility. In fact, melanosomes still undergo rapid bi-directional, microtubule dependent movements between the center and the periphery of melanocytes in those mutant cells (Barral and Seabra, 2004). The trafficking and processing of proteins that influence melanin synthesis (e.g. tyrosinase) and the structure (e.g. Pmel17) of melanosomes appear not to be affected by those mutations. It should also be noted that early melanosomes need to remain in the perinuclear area until delivery of enzymatic and structural components required for their function is complete. Thus a wide range of regulatory factors and mechanisms remain to be identified that control melanosome maturation in the perinuclear region of melanocytic cells and prevent their dispersion to the dendrites of the cells until they are sufficiently mature. A schematic summarizing these processes and the findings of this study is presented in Figure 8.

Our recently published proteomics analysis (Chi et al., 2006) allowed us to compare early and late melanosomes in pigmented and in unpigmented melanocytic cells. Microtubule-dependent intracellular transport is mediated by motor proteins of the kinesin and of the cytoplasmic dynein superfamilies (Chen et al., 2005). Interestingly, dynein is the common motor protein found in early melanosomes, not kinesin. Dynein has a well established role in the localization and movement of diverse types of cargo, including late endosomes and lysosomes (Valetti et al., 1999). Dynein also plays a significant role as an early endosomal motor and it contributes directly to endosomal fusion, particularly in receptor sorting (Driskell et al., 2007). Further,

the confirmation of spectrin to be present in human melanosomes is novel and highly important. Our results suggest that spectrin is involved in the aggregation of early melanosomes, but not in their dispersion, due to its centralized distribution (not in dendrites) in melanocytic cells. It is possible that in amphibian melanophores, spectrin may be involved in both processes (Aspengren and Wallin, 2004). Interestingly, the spectrin/ankyrin skeleton is involved in cargo selection and in the interaction with clathrin coated pits in endocytosis which tether either microfilaments or microtubules (De Matteis and Morrow, 2000). Therefore, the intracellular distribution of spectrin and the relationship with pigment granules in melanocytic cells suggests a role for the spectrin skeleton to deliver cargo vesicles to target organelles.

Our results showing that movement of early melanosomes is dominated by dyneins and spectrin is novel and is consistent with the ongoing maturation process these organelles undergo. These results are also consistent with the fact that only pigmented “mature' melanosomes bind to microtubules for transport to the cell periphery prior to their transfer to keratinocytes. In fact, early melanosomes need to be “anchored' in the perinuclear area to receive sorting vesicles containing critical melanosomal proteins needed for their maturation and eventually for pigment biosynthesis. Our hypothesis is supported by the fact that intermediate filaments may physically hinder organelles in place by making transport more difficult for molecular motors in vivo (Kural et al., 2007). Apparently, microtubule-mediated transport of early and late melanosomes may be regulated by the relative amount of two Rab proteins, Rab7 and Rab27a (Jordens et al., 2006).

Physiological regulation of melanosome transport by αMSH has been reported previously in amphibian melanophores (Deacon et al., 2003). In mammalian cells, murine melanocytes represent the best model to evaluate the effects of αMSH and its inverse agonist counterpart, ASP. Therefore, our results further reveal that the expression of motor proteins can indeed be physiologically regulated by those pigmentary hormones. The results obtained with αMSH are consistent with its role in stimulating pigmentation. The results obtained with ASP are novel and interesting, and in this regard, it has been reported that ASP decreases pigmentation. The role of ASP to down-regulate the expression of genes encoding melanosomal proteins (Sakai et al., 1997) or decrease melanosome maturation (Suzuki et al., 1997) in normal melanocytes has been previously shown. However, our novel results further indicate that ASP also disrupts the transport of early melanosomes. These results are consistent with the current view that over-expression of ASP promotes the dedifferentiation of melanocytes (Sviderskaya et al., 2001).

Finally, processing of TYR but not Pmel17 to melanosomes is affected by genetic alterations in the endocytic pathway, as observed in Hermansky- Pudlak Syndrome (reviewed in (Huizing et al., 2001)). This suggests the existence of alternative pathways at later steps of the secretory pathway to reach melanosomes. Using SK-Mel-28 cells as a model, we have confirmed that small amounts of TYR and Pmel17 sort through the plasma membrane to reach their intracellular targets. Further, the presence of AP2 in melanosomes, which is also found in the plasma membrane, is consistent with that finding. However, sorting of TYR to melanosomes is less efficient than Pmel17 using that pathway. Apparently, TYR uses AP1 and AP3 to sort through the endocytic pathway (Theos et al., 2005). These results are also consistent with our recent report that Pmel17 uses AP2 and AP1 to reach melanosomes in pigmented melanoma cells or in unpigmented melanocytic cells (Valencia et al., 2006). Our results further complement these studies since it evaluates the sorting of TYR via an alternate pathway which does not seem to be used in pigmented melanoma cells.

MATERIALS AND METHODS

Cell Cultures

SK-Mel-28 unpigmented human melanoma cells were cultured in minimum essential medium (GIBCO, Grand Island, NY, USA) containing 10% fetal bovine serum (FBS), as described previously (Watabe et al., 2004). MNT-1 pigmented human melanoma cells were cultured in Dulbecco's modified Eagle medium (DMEM, GIBCO) containing 20% FBS, as described previously (Kushimoto et al., 2001). Melan-a melanocytes, derived from C57BL/6J nonagouti black mice (gift from Prof. Dorothy C. Bennett, St. George's Hospital Medical School, London, UK) were cultured at 37 °C with 5% CO_2 in RPMI 1640 medium (GIBCO) containing 5% fetal bovine serum (Atlanta Biologicals, Norcross, GA, USA), 7.5% sodium bicarbonate (GIBCO), 200 nM 2-o-tetradecanoylphorbol-13-acetate (Sigma, St Louis, MO, USA), 100 μM 2-mercaptoethanol (Sigma), penicillin and streptomycin (GIBCO), and L-glutamine (GIBCO) at pH 7.2. Where noted, melan-a melanocytes were cultured for 3 days with or without 100 nM αMSH (Sigma) or 1 nM ASP as previously described (Sakai et al., 1997).

Antibodies and Reagents

αPEP7h and αPEP13h antibodies were generated in rabbits against synthetic peptides corresponding to the carboxyl termini of human TYR and Pmel17, respectively, as previously described (Jiménez et al., 1991; Kobayashi et al., 1994). Monoclonal antibodies against kinesin, spectrin, cytoplasmic dynein and β-actin were purchased from AbCam (Cambridge, UK). Other antibodies used to localize subcellular organelles and cytoskeletal components were as follows: calnexin (ER) from BD Transduction Laboratories (Lexington, KY, USA), vATPase and β-tubulin (microtubules) from Santa Cruz Biotechnology (Santa Cruz, CA, USA), and rhodamine phalloidin (actin filaments) from Molecular Probes (Eugene, OR, USA). Bafilomycin and brefeldin A were purchased from Sigma. Nocodazole and cytochalasin D were purchased from Calbiochem (San Diego, CA, USA). EndoH was from New England Biolabs (Beverly, MA, USA).

Immunofluorescence Microscopy

For observation using confocal microscopy, cells were plated and cultured in 2-well Lab-Tek chamber slides (Nalge Nunc Intl, Naperville, IL, USA) and were then stained by double indirect immunofluorescence methods, as described previously (Valencia et al., 2006). After washing in PBS, cells were fixed in 4% paraformaldehyde at 4°C. Cells were then permeabilized with 0.01% Triton-X100 for 3 min at 23°C and were blocked with a solution containing 5% normal goat serum and 5% normal horse serum for 1 hr at 23°C. Cells were incubated with primary antibodies (at dilutions noted in the Figure legends) overnight at 4°C. Goat anti-rabbit IgG labeled with Texas red and horse anti-mouse IgG labeled with fluorescein (1:100; Vector, Burlingame, CA, USA) were used to detect polyclonal and monoclonal antibodies, respectively. Nuclear counterstaining was done with DAPI (Vector). Reactivity was classified into three categories, according to whether they showed green, red, or yellow fluorescence; the latter was indicative of colocalization of the red and green fluorescence signals. All preparations were examined with a Zeiss LSM 510 confocal microscope (Zeiss, Jena, Germany), equipped with HeNe, argon, krypton and UV laser sources. To visually observe the acidity of intracellular compartments, cells were incubated for 20 min at 37°C in MEM with 5 μg/ml acridine orange (Fuller et al., 2001). After extensive washing with PBS, coverslips were mounted onto slides. Fluorescence was observed using a Leica DMR B/D MLD fluorescence microscope (Leica Microsystems, Bannockburn, IL, USA).

Western Blotting

Cell extracts were prepared for SDS-PAGE analysis as described previously (Watabe et al., 2004). Briefly, cell extracts were mixed in Tris-glycine SDS sample buffer (2x) (Invitrogen, Carlsbad, CA, USA) supplemented with 2-mercaptoethanol (2-ME) and boiled for 5 min. Samples (10 μg protein/well) were loaded into 8% or 8% -16% gradient SDS-PAGE gels (Invitrogen) and were then transferred to Immobilon-P membranes (Millipore, Bedford, MA, USA). Membranes were placed in blocking solution (5% non-fat dry milk in 10 mM Tris-HCl, pH 7.2; 150 mM NaCl; 1% Tween 20) for 1 hr at 23°C and were then incubated with primary antibodies (diluted as noted in the Figure legends) overnight at 4°C. Membranes were incubated in horseradish peroxidase-linked anti-rabbit, anti-mouse whole antibodies (1:1000) (Amersham, Piscataway, NJ, USA) or anti-goat immunoglobulin (DAKO, Carpinteria, CA, USA) for 1 hr at 23°C. Bound antibodies were detected using an ECL-plus Detection System (Amersham) according to the manufacturer's instructions.

Electron microscopy and DOPA staining

This procedure was performed as reported previously (Kushimoto et al., 2001). Briefly, cells were harvested in PBS and fixed in 2% glutaraldehyde, 2% paraformaldehyde in 0.1 M sodium cacodylate buffer (pH 7.3). Samples were then stained with 0.1% L-DOPA (Sigma) for 2 hr and were washed with 0.1 M cacodylate buffer. Samples were then embedded in epoxy resin. Thin sections were cut, stained with uranyl acetate and then examined with a Zeiss EM 912 EX electron microscope.

Glycosidase Digestion

Cell extracts (2 μg protein) were digested with 1000 U EndoH for 3 hr at 37°C. After digestion, extracts were subjected to SDS-PAGE as described above.

Metabolic Labeling and Immunoprecipitation

Metabolic labeling and immunoprecipitation was performed as described previously (Costin et al., 2003). Briefly, cells were incubated in Met/Cys-free DMEM medium containing 10% dialyzed fetal bovine serum (GIBCO) for 30 min at 37°C and were then labeled for 30 min at 37°C with 0.5 mCi of [^{35}S]-Met/Cys (Amersham). Cells were chased at various times at 37° C (as detailed in the Figure legends) in medium supplemented with 1 mM methionine. At this time, cells were treated where indicated with 10 μg/ml brefeldin A, 10 μg/ml nocodazole or 10 mg/ml cytochalasin D. Cells were harvested and solubilized overnight at 4°C in lysis buffer (50 mM Tris-HCl, pH 7.4, 150 mM NaCl, 1% NP-40, 0.01% SDS, containing complete protease inhibitor cocktail). Cell extracts were cleared for 2 hr at 4°C first with normal rabbit serum (Vector) and then with Protein-G Sepharose beads (Amersham). Proteins were immunoprecipitated with either αPEP7h or αPEP13h and complexes were separated with Protein-G Sepharose beads for 2 hr at 4°C. Pellets were prepared for SDS-PAGE analysis as described above.

Subcellular fractionation

Isolation of melanosomes, clathrin-coated vesicles and endosomes were done as described previously without modifications (Watabe et al., 2004). Purification of plasma membranes by the sucrose and iodixonadol gradients was performed as described previously, also without modifications (Valencia et al., 2006).

Microarray Hybridization and Data Analysis

The detailed procedure for DNA μarray analysis used is available at http://nciarray.nci.nih.gov/reference/NCIReference.shtml. Briefly, 10 μg total RNA, isolated using an Rneasy Mini Kit

(Qiagen, Valencia, CA, USA), from αMSH- or ASP-treated or from untreated melan-a melanocytes were used to derive fluorescently (Cy5 or Cy3) labeled cDNAs which were hybridized on Mouse Exonic Evidence Based Oligonucleotide (MEEBO) arrays. These arrays contain a genome-wide set (>38K) of long-mer mouse oligonucleotides and were manufactured and printed at the Advanced Technology Center (National Cancer Institute, Gaithersburg, MD, USA). At least two hybridizations were performed for each of the 3 biological replicates using a dye-swap strategy to eliminate labeling bias of the fluorescent intensity measurement. Hybridized arrays were scanned at 10 μm resolution on a GenePix 4000B microarray scanner running GenePix 5.0 software (Axon instruments, Union City, CA, USA) at variable photomultiplier tube voltage to obtain the maximal signal intensities with 1% probe saturation. Another scan was performed at a lower pmt to avoid any saturated spot in order to get the complete set of altered genes. For each spot, the highest value of each non-saturated spot was used. Array data (images and sample intensity files) were entered into the NCI microarray database (mAdb, http://nciarray.nci.nih.gov/index.shtml), to be filtered and normalized. Our quality filter required each spot to have a signal to background ratio of at least 2 for one of the two channels and at least 50 foreground pixels. Cy3:Cy5 intensity ratios were normalized by median centering of ratios for each array. After inverting the ratios of the reciprocal experiment, the data were transformed to logarithmic scale to the base 2 for statistical calculations. Differentially expressed genes between αMSH- or ASP-treated versus control samples were identified using one sample t-tests. Treated-to-control sample ratios were calculated using geometric averages of the replicates. Changes in gene expression are considered significant (at $p \leq 0.01$) when up- or down-regulated by at least 1.5-fold by ASP and/or by αMSH, after averaging the replicates, and data were present at least for half of the 6 replicates. Global expression changes are considered to be statistically significant since the number of genes differentially expressed at $p < 0.01$ were found to be about 5-fold larger than estimated false discoveries at this p-value.

ACKNOWLEDGEMENTS

This research was supported in part by the Intramural Research Program of the NIH, National Cancer Institute, Center for Cancer Research.

Abbreviations

AP, adaptor protein; Baf, bafilomycin A1; COP, coat protein; CV, coated vesicle; EndoH, endoglycosidase H; ER, endoplasmic reticulum; TYR, tyrosinase; vATPase, vacuolar type proton ATPase.

REFERENCES

Abdel-Malek ZA, Scott MC, Furumura M, Lamoreux ML, Ollmann M, Barsh GS, Hearing VJ. The melanocortin 1 receptor is the principal mediator of the effects of agouti signaling protein on mammalian melanocytes. J Cell Sci 2001;114:1019–1024. [PubMed: 11181184]

Aspengren S, Wallin M. A role for spectrin in dynactin-dependent melanosome transport in Xenopus laevis melanophores. Pigment Cell Res 2004;17:295–301. [PubMed: 15140076]

Aunis D, Bader MF. The cytoskeleton as a barrier to exocytosis in secretory cells. J Exp Biol 1988;139:253–266. [PubMed: 3062121]

Barral DC, Seabra MC. The melanosome as a model to study organelle motility in mammals. Pigment Cell Res 2004;17:111–118. [PubMed: 15016299]

Ben-Tekaya H, Miura K, Pepperkok R, Hauri HP. Live imaging of bidirectional traffic from the ERGIC. J Cell Sci 2005;118:357–367. [PubMed: 15632110]

Broderick MJ, Winder SJ. Spectrin, alpha-actinin, and dystrophin. Adv Protein Chem 2005;70:203–246. [PubMed: 15837517]

Byers HR, Yaar M, Eller MS, Jalbert N, Gilchrest BA. Role of cytoplasmic dynein in melanosome transport in human melanocytes. J Invest Dermatol 2000;114:990–997. [PubMed: 10771482]

Chen JL, Fucini RV, Lacomis L, Erdjument-Bromage H, Tempst P, Stamnes M. Coatomer-bound Cdc42 regulates dynein recruitment to COPI vesicles. J Cell Biol 2005;169:383–389. [PubMed: 15866890]

Chen SH, Bubb MR, Yarmola EG, Zuo J, Jiang J, Lee BS, Lu M, Gluck SL, Hurst IR, Holliday LS. Vacuolar H+-ATPase binding to microfilaments: regulation in response to phosphatidylinositol 3-kinase activity and detailed characterization of the actin-binding site in subunit B. J Biol Chem 2004;279:7988–7998. [PubMed: 14662773]

Chi A, Valencia JC, Hu ZZ, Watabe H, Yamaguchi H, Mangini N, Huang H, Canfield VA, Cheng KC, Yang F, Abe R, Yamagishi S, Shabanowitz J, Hearing VJ, Wu CH, Appella E, Hunt DF. Proteomic and bioinformatic characterization of the biogenesis and function of melanosomes. J Prot Res 2006;5:3135–3144.

Costin GE, Valencia JC, Vieira WD, Lamoreux ML, Hearing VJ. Tyrosinase processing and intracellular trafficking is disrupted in mouse primary melanocytes carrying the uw mutation: a model for oculocutaneous albinism (OCA) type 4. J Cell Sci 2003;116:3203–3212. [PubMed: 12829739]

De Matteis MA, Morrow JS. Spectrin tethers and mesh in the biosynthetic pathway. J Cell Sci 2000;113 (Pt 13):2331–2343. [PubMed: 10852813]

Deacon SW, Serpinskaya AS, Vaughan PS, Fanarraga ML, Vernos I, Vaughan KT, Gelfand VI. Dynactin is required for bidirectional organelle transport. J Cell Biol 2003;160:297–301. [PubMed: 12551954]

Driskell OJ, Mironov A, Allan VJ, Woodman PG. Dynein is required for receptor sorting and the morphogenesis of early endosomes. Nat Cell Biol 2007;9:113–120. [PubMed: 17173037]

Francis E, Wang N, Parag H, Halaban R, Hebert DN. Tyrosinase maturation and oligomerization in the endoplasmic reticulum require a melanocyte-specific factor. J Biol Chem 2003;278:25607–25617. [PubMed: 12724309]

Fuller BB, Spaulding DT, Smith DR. Regulation of the catalytic activity of preexisting tyrosinase in Black and Caucasian human melanocyte cell cultures. Exp Cell Res 2001;262:197–208. [PubMed: 11139343]

Furumura M, Sakai C, Abdel-Malek ZA, Barsh GS, Hearing VJ. The interaction of agouti signal protein and melanocyte stimulating hormone to regulate melanin formation in mammals. Pigment Cell Res 1996;9:191–203. [PubMed: 8948501]

Godi A, Santone I, Pertile P, Devarajan P, Stabach PR, Morrow JS, Di TG, Polishchuk R, Petrucci TC, Luini A, De Matteis MA. ADP ribosylation factor regulates spectrin binding to the Golgi complex. Proc Natl Acad Sci U S A 1998;95:8607–8612. [PubMed: 9671725]

Gross SP, Tuma MC, Deacon SW, Serpinskaya AS, Reilein AR, Gelfand VI. Interactions and regulation of molecular motors in Xenopus melanophores. J Cell Biol 2002;156:855–865. [PubMed: 11864991]

Halaban R, Cheng E, Zhang Y, Moellmann G, Hanlon DP, Michalak M, Vijayasaradhi S, Hebert DN. Aberrant retention of tyrosinase in the endoplasmic reticulum mediates accelerated degradation of the enzyme and contributes to the dedifferentiated phenotype of amelanotic melanoma cells. Proc Natl Acad Sci USA 1997;94:6210–6215. [PubMed: 9177196]

Halaban R, Patton RS, Cheng E, Svedine S, Trombetta ES, Wahl ML, Ariyan S, Hebert DN. Abnormal acidification of melanoma cells induces tyrosinase retention in the early secretory pathway. J Biol Chem 2002;277:14821–14828. [PubMed: 11812790]

Hara M, Yaar M, Byers HR, Goukassian DA, Fine RE, Gonsalves J, Gilchrest BA. Kinesin participates in melanosomal movement along melanocyte dendrites. J Invest Dermatol 2000;114:438–443. [PubMed: 10692101]

Hearing VJ. The melanosome: the perfect model for cellular responses to the environment. Pigment Cell Res 2000;13:23–34. [PubMed: 11041354]

Hearing VJ, Ekel TM. Mammalian tyrosinase: A comparison of tyrosine hydroxylation and melanin formation. Biochem J 1976;157:549–557. [PubMed: 825109]

Huizing M, Anikster Y, Gahl WA. Hermansky-Pudlak syndrome and Chediak-Higashi syndrome: disorders of vesicle formation and trafficking. Thromb Haemost 2001;86:233–245. [PubMed: 11487012]

Jiménez M, Tsukamoto K, Hearing VJ. Tyrosinases from two different loci are expressed by normal and by transformed melanocytes. J Biol Chem 1991;266:1147–1156. [PubMed: 1898730]

Jordens I, Westbroek W, Marsman M, Rocha N, Mommaas AM, Huizing M, Lambert J, Naeyaert JM, Neefjes J. Rab7 and Rab27a control two motor protein activities involved in melanosomal transport. Pigment Cell Res 2006;19:412–423. [PubMed: 16965270]

Kobayashi T, Urabe K, Orlow SJ, Higashi K, Imokawa G, Kwon BS, Potterf SB, Hearing VJ. The pmel17/*silver* locus protein: characterization and investigation of its role in mammalian melanogenesis. J Biol Chem 1994;269:29198–29205. [PubMed: 7961886]

Körner AM, Pawelek JM. Mammalian tyrosinase catalyzes three reactions in the biosynthesis of melanin. Science 1982;217:1163–1165. [PubMed: 6810464]

Kural C, Serpinskaya AS, Chou YH, Goldman RD, Gelfand VI, Selvin PR. Tracking melanosomes inside a cell to study molecular motors and their interaction. Proc Natl Acad Sci U S A 2007;104:5378–5382. [PubMed: 17369356]

Kushimoto T, Basrur V, Valencia JC, Matsunaga J, Vieira WD, Muller J, Appella E, Hearing VJ. A new model for melanosome biogenesis based on the purification and mapping of early melanosomes. Proc Natl Acad Sci USA 2001;98:10698–10703. [PubMed: 11526213]

Kushimoto T, Valencia JC, Costin GE, Toyofuku K, Watabe H, Yasumoto K, Rouzaud F, Vieira WD, Hearing VJ. The Seiji Memorial Lecture - The melanosome: an ideal model to study cellular differentiation. Pigment Cell Res 2003;16:237–244. [PubMed: 12753396]

Lambert J, Vancoillie G, Naeyaert JM. Molecular motors and their role in pigmentation. Cell Mol Biol 1999;45:905–918. [PubMed: 10643995]

Lazaro-Dieguez F, Jimenez N, Barth H, Koster AJ, Renau-Piqueras J, Llopis JL, Burger KN, Egea G. Actin filaments are involved in the maintenance of Golgi cisternae morphology and intra-Golgi pH. Cell Motil Cytoskeleton 2006;63:778–791. [PubMed: 16960891]

Logan DW, Burn SF, Jackson IJ. Regulation of pigmentation in zebrafish melanophores. Pigment Cell Res 2006;19:206–213. [PubMed: 16704454]

Lopes VS, Ramalho JS, Owen DM, Karl MO, Strauss O, Futter CE, Seabra MC. The ternary Rab27a-Myrip-Myosin VIIa complex regulates melanosome motility in the retinal pigment epithelium. Traffic 2007;8:486–499. [PubMed: 17451552]

Michaely P, Kamal A, Anderson RG, Bennett V. A requirement for ankyrin binding to clathrin during coated pit budding. J Biol Chem 1999;274:35908–35913. [PubMed: 10585476]

Oetting WS, Fryer JP, Shriram S, King RA. Oculocutaneous albinism type 1: the last 100 years. Pigment Cell Res 2003;16:307–311. [PubMed: 12753405]

Presley JF, Cole NB, Schroer TA, Hirschberg K, Zaal KJ, Lippincott-Schwartz J. ER-to-Golgi transport visualized in living cells. Nature 1997;389:81–85. [PubMed: 9288971]

Robertson AM, Allan VJ. Brefeldin A-dependent membrane tubule formation reconstituted *in vitro* is driven by a cell cycle-regulated microtubule motor. Mol Biol Cell 2000;11:941–955. [PubMed: 10712511]

Sakai C, Ollmann M, Kobayashi T, Abdel-Malek ZA, Muller J, Vieira WD, Imokawa G, Barsh GS, Hearing VJ. Modulation of murine melanocyte function in vitro by agouti signal protein. EMBO J 1997;16:3544–3552. [PubMed: 9218796]

Salas PJ, Misek DE, Vega-Salas DE, Gundersen D, Cereijido M, Rodriguez-Boulan E. Microtubules and actin filaments are not critically involved in the biogenesis of epithelial cell surface polarity. J Cell Biol 1986;102:1853–1867. [PubMed: 2871031]

Schnapp BJ, Reese TS. Dynein is the motor for retrograde axonal transport of organelles. Proc Natl Acad Sci U S A 1989;86:1548–1552. [PubMed: 2466291]

Suzuki I, Tada A, Ollmann M, Barsh GS, Im S, Lamoreux ML, Hearing VJ, Nordlund JJ, Abdel-Malek ZA. Agouti signalling protein inhibits melanogenesis and the response of human melanocytes to α-melanotropin. J Invest Dermatol 1997;108:838–842. [PubMed: 9182807]

Sviderskaya EV, Hill SP, Balachandar D, Barsh GS, Bennett DC. Agouti signaling protein and other factors modulating differentiation and proliferation of immortal melanoblasts. Devel Dynam 2001;221:373–379.

Taoka M, Ichimura T, Wakamiya-Tsuruta A, Kubota Y, Araki T, Obinata T, Isobe T. V-1, a protein expressed transiently during murine cerebellar development, regulates actin polymerization via interaction with capping protein. J Biol Chem 2003;278:5864–5870. [PubMed: 12488317]

Theos AC, Tenza D, Martina JA, Hurbain I, Peden AA, Sviderskaya EV, Stewart A, Robinson MS, Bennett DC, Cutler DF, Bonifacino JS, Marks MS, Raposo G. Functions of adaptor protein (AP)-3 and AP-1 in tyrosinase sorting from endosomes to melanosomes. Mol Biol Cell 2005;16:5356–5372. [PubMed: 16162817]

Toyofuku K, Wada I, Valencia JC, Kushimoto T, Ferrans VJ, Hearing VJ. Oculocutaneous albinism (OCA) types 1 and 3 are ER retention diseases: Mutations in tyrosinase and/or Tyrp1 influence the maturation, degradation of calnexin association of the other. FASEB J 2001;15:2149–2161. [PubMed: 11641241]

Ujvari A, Aron R, Eisenhaure T, Cheng E, Parag H, Smicun Y, Halaban R, Hebert DN. Translation rate of human tyrosinase determines its N-linked glycosylation level. J Biol Chem 2001;276:5924–5931. [PubMed: 11069924]

Valderrama F, Duran JM, Babia T, Barth H, Renau-Piqueras J, Egea G. Actin microfilaments facilitate the retrograde transport from the Golgi complex to the endoplasmic reticulum in mammalian cells. Traffic 2001;2:717–726. [PubMed: 11576448]

Valencia JC, Rouzaud F, Julien S, Chen KG, Passeron T, Yamaguchi Y, Abu-Asab M, Tsokos M, Costin GE, Yamaguchi H, Jenkins LM, Nagashima K, Appella E, Hearing VJ. Sialylated core 1 O-glycans influence the sorting of Pmel17/gp100 and determine its capacity to form fibrils. J Biol Chem 2007;282:11266–11280. [PubMed: 17303571]

Valencia JC, Watabe H, Chi A, Rouzaud F, Chen KG, Vieira WD, Takahashi K, Yamaguchi Y, Berens W, Nagashima K, Shabanowitz J, Hunt DF, Appella E, Hearing VJ. Sorting of Pmel17 to melanocytes through the plasma membrane by AP1 and AP2: evidence for the polarized nature of melanocytes. J Cell Sci 2006;119:1080–1091. [PubMed: 16492709]

Valetti C, Wetzel DM, Schrader M, Hasbani MJ, Gill SR, Kreis TE, Schroer TA. Role of dynactin in endocytic traffic: effects of dynamitin overexpression and colocalization with CLIP-170. Mol Biol Cell 1999;10:4107–4120. [PubMed: 10588646]

Vallee RB, Wall JS, Paschal BM, Shpetner HS. Microtubule-associated protein 1C from brain is a two-headed cytosolic dynein. Nature 1988;332:561–563. [PubMed: 2965791]

Vancoillie G, Lambert J, Haeghen YV, Westbroek W, Mulder A, Koerten HK, Mommaas AM, van Oostveldt P, Naeyaert JM. Colocalization of dynactin subunits P150Glued and P50 with melanosomes in normal human melanocytes. Pigment Cell Res 2000a;13:449–457. [PubMed: 11153697]

Vancoillie G, Lambert JM, Mulder A, Koerten HK, Mommaas AM, van Oostveldt P, Naeyaert JM. Cytoplasmic dynein colocalizes with melanosomes in normal human melanocytes. Brit J Dermatol 2000b;143:298–306. [PubMed: 10951136]

Vitavska O, Wieczorek H, Merzendorfer H. A novel role for subunit C in mediating binding of the H+-V-ATPase to the actin cytoskeleton. J Biol Chem 2003;278:18499–18505. [PubMed: 12606563]

Watabe H, Valencia JC, Yasumoto K, Kushimoto T, Ando H, Muller J, Vieira WD, Mizoguchi M, Appella E, Hearing VJ. Regulation of tyrosinase processing and trafficking by organellar pH and by proteasome activity. J Biol Chem 2004;279:7971–7981. [PubMed: 14634018]

Wu X, Hammer JA III. Making sense of melanosome dynamics in mouse melanocytes. Pigment Cell Res 2000;13:241–247. [PubMed: 10952391]

Wu X, Sakamoto T, Zhang F, Sellers JR, Hammer JA. In vitro reconstitution of a transport complex containing Rab27a, melanophilin and myosin Va. FEBS Lett 2006;580:5863–5868. [PubMed: 17045265]

Wu XS, Rao K, Zhang H, Wang F, Sellers JR, Matesic LE, Copeland NG, Jenkins NA, Hammer JA. Identification of an organelle receptor for myosin-Va. Nature Cell Biol 2002;4:271–278. [PubMed: 11887186]

Zagon IS, Higbee R, Riederer BM, Goodman SR. Spectrin subtypes in mammalian brain: an immunoelectron microscopic study. J Neurosci 1986;6:2977–2986. [PubMed: 3531427]

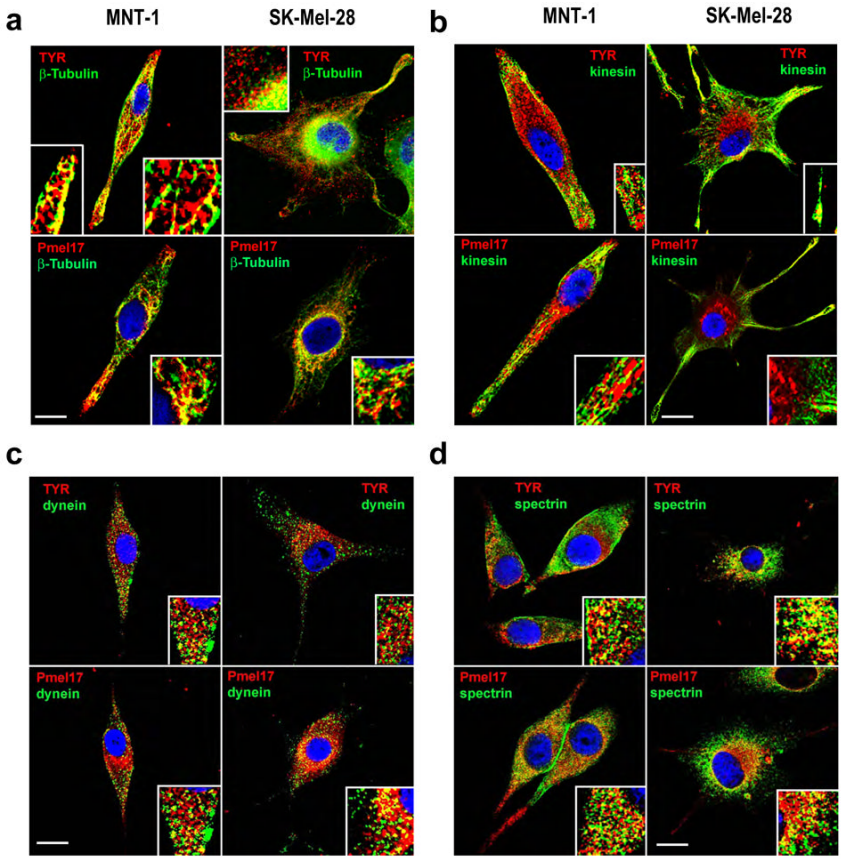

Figure 1. Subcellular localization of TYR and Pmel17 in relation to microtubules, motor proteins and spectrin

MNT-1 cells and SK-Mel-28 cells were fixed and stained with antibodies recognizing TYR (αPEP7h at 1:40) and Pmel17 (αPEP13h at 1:40), both in red, as well as markers for microtubules **(A)** (β-tubulin at 1:10), kinesin **(B,** 1:250**),** dynein **(C,** 1:250**)** and spectrin **(D,** 1:100**)**, all in green. Subcellular localization was examined by confocal microscopy. Insets show higher magnifications of perinuclear or dendrite areas in each panel. Nuclei were counterstained with DAPI (blue). Representative images from two separate experiments are shown for each combination of antibodies. Scale bars = 10 μm

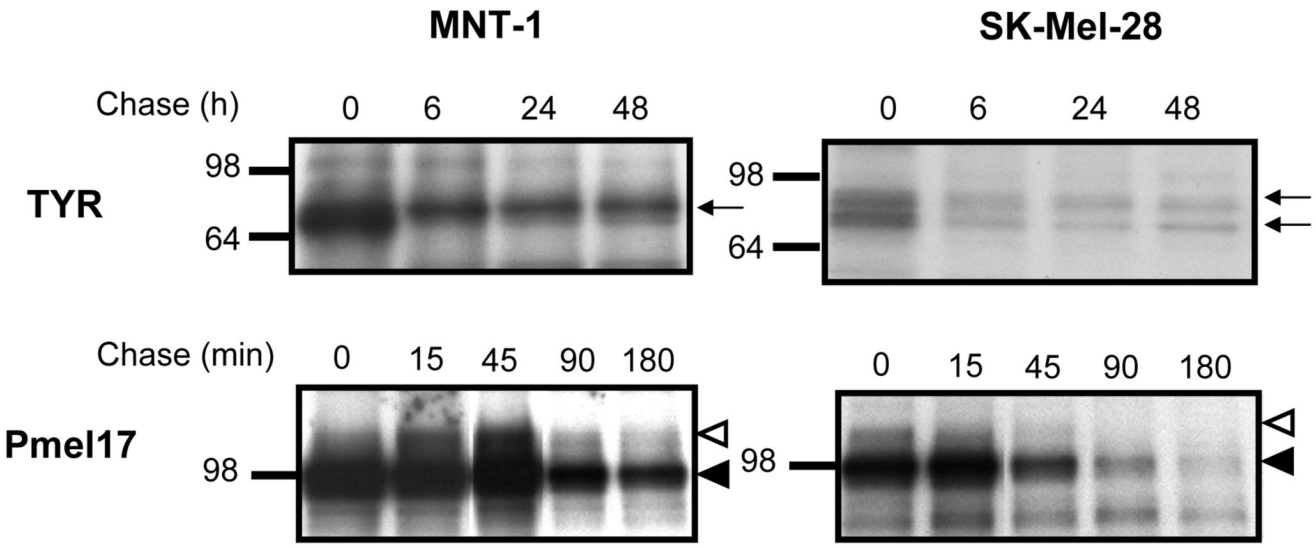

Figure 2. Processing and ultrastructural localization of TYR and Pmel17 in melanoma cells

A) MNT-1 and SK-Mel-28 cells were [^{35}S] metabolically labeled for 30 min and were chased for times indicated after which samples were immunoprecipitated with αPEP7h or αPEP13h as noted. Immunoreactive bands were visualized by autoradiography. Molecular weight markers are indicated on the left in kDa.

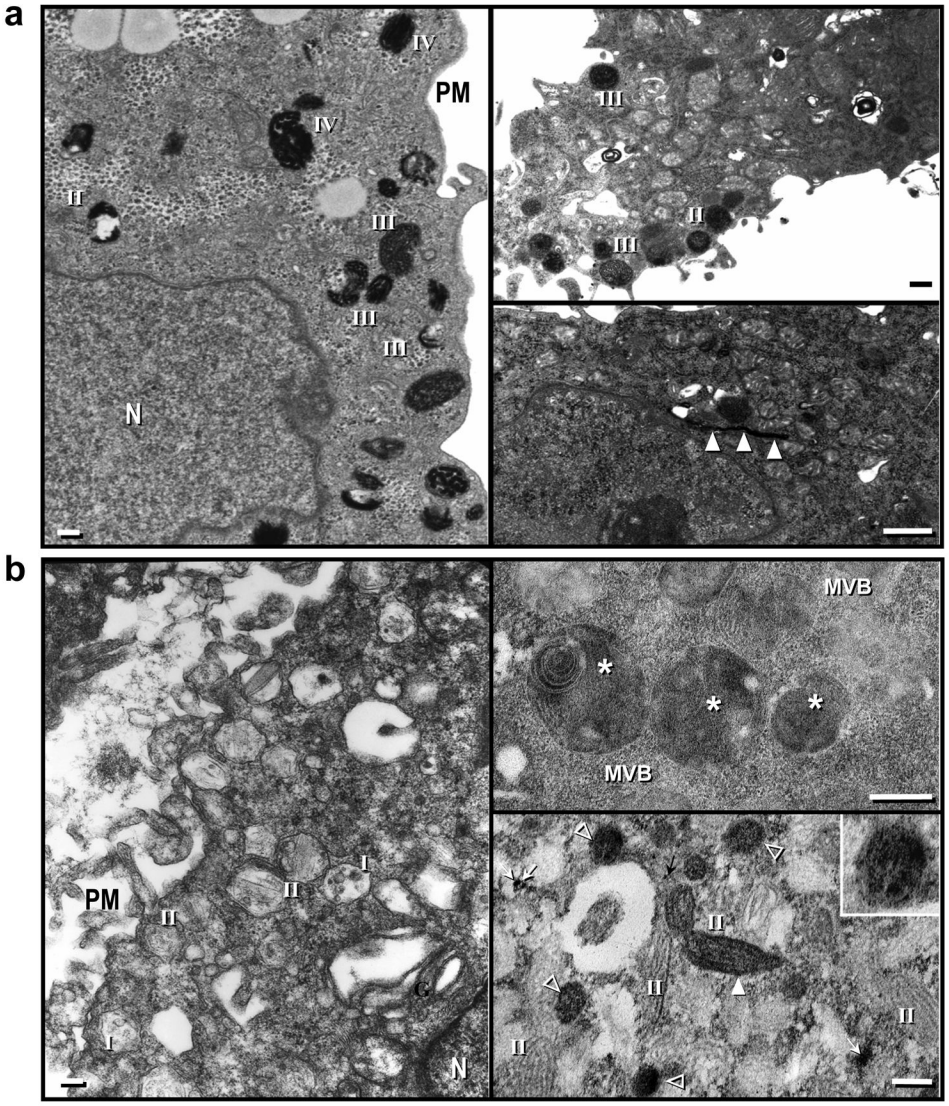

Figure 3.

Electron micrographs showing the predominant amounts of late stage (III and IV) melanosomes in MNT-1 cells (**A**) and stage II over stage I melanosomes in SK-Mel-28 cells (**D**). Electron micrographs of MNT-1 cells treated with DOPA to demonstrate the presence of functional tyrosinase inside stage II and III melanosomes (**B**) or sometimes inside Golgi stacks (**C**; open arrows). Electron micrograph of SK-Mel-28 cells treated with DOPA to demonstrate the presence of functional tyrosinase inside multivesicular bodies (**E**; asterisks) or inside other intracellular organelles **(F)** such as stage II melanosomes (closed arrowheads), rounded vesicles (open arrowheads) or small vesicles (arrows). Inset shows high power image of a DOPA-positive vesicle without visible fibrils. Note that most stage II melanosomes are not stained with DOPA. Roman numbers indicate melanosome stages. PM: plasma membrane; N: nuclei; G: Golgi.

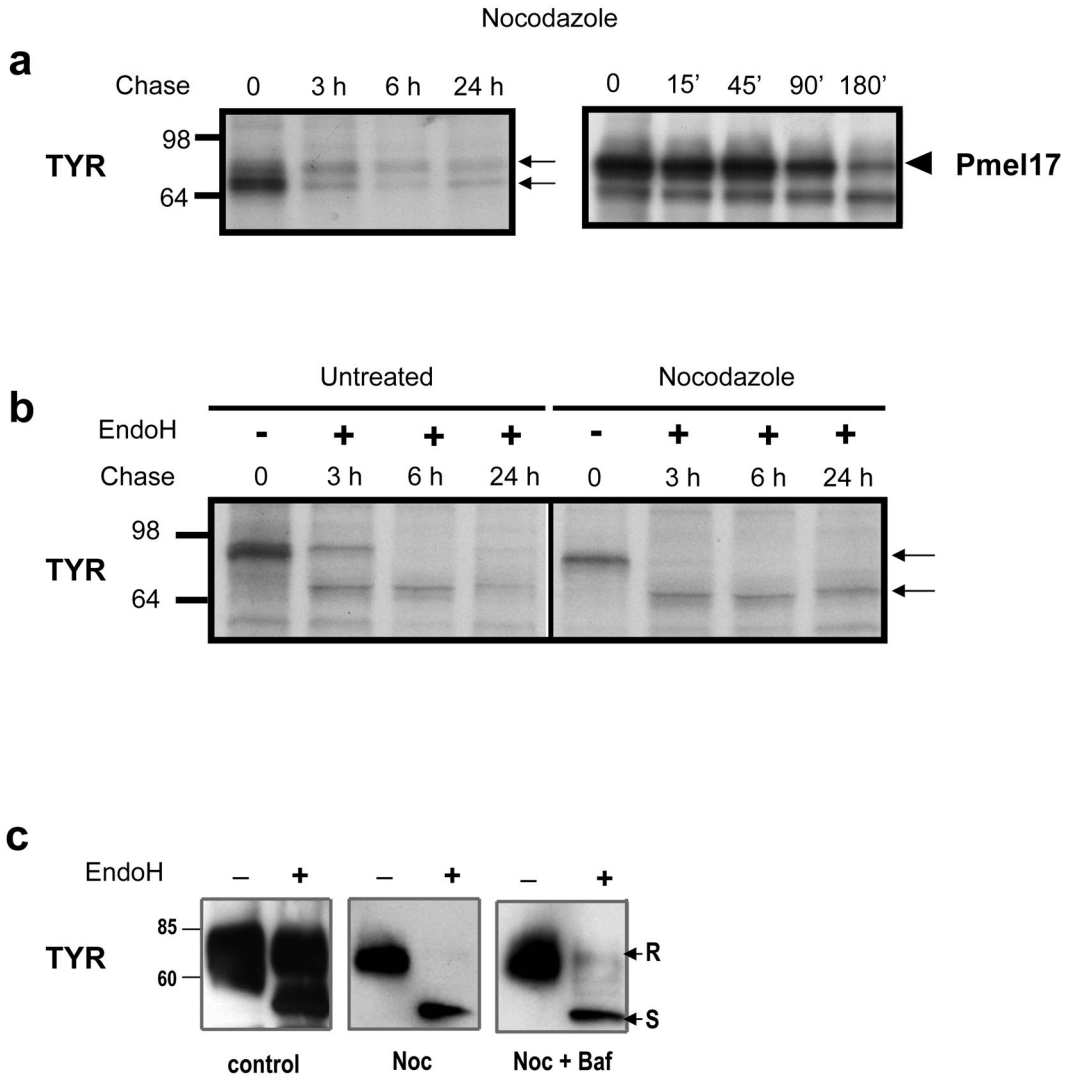

Figure 4. TYR and Pmel17 trafficking depends on microtubules

(A and B) SK-Mel-28 cells were pretreated with 10 mg/ml nocodazole for 3 hr and then were metabolically labeled with [^{35}S] for 30 min. The cells were then chased for the times indicated and were immunoprecipitated with antibodies against TYR or Pmel17 as noted. **(B)** Immunoprecipitates from untreated or nocodazole-treated samples collected after 0 hr chase were digested with EndoH where noted. **(C)** SK-Mel-28 cells were left untreated or were treated with nocodazole or nocodazole plus bafilomycin A for 3 hr before harvest. Cell extracts were then digested with or without EndoH, and TYR was detected by Western blot. Arrows indicate EndoH resistant ("R") and sensitive ("S") bands. Immunoreactive bands for metabolic labeling were visualized by autoradiography. Molecular weight markers are indicated on the left in kDa.

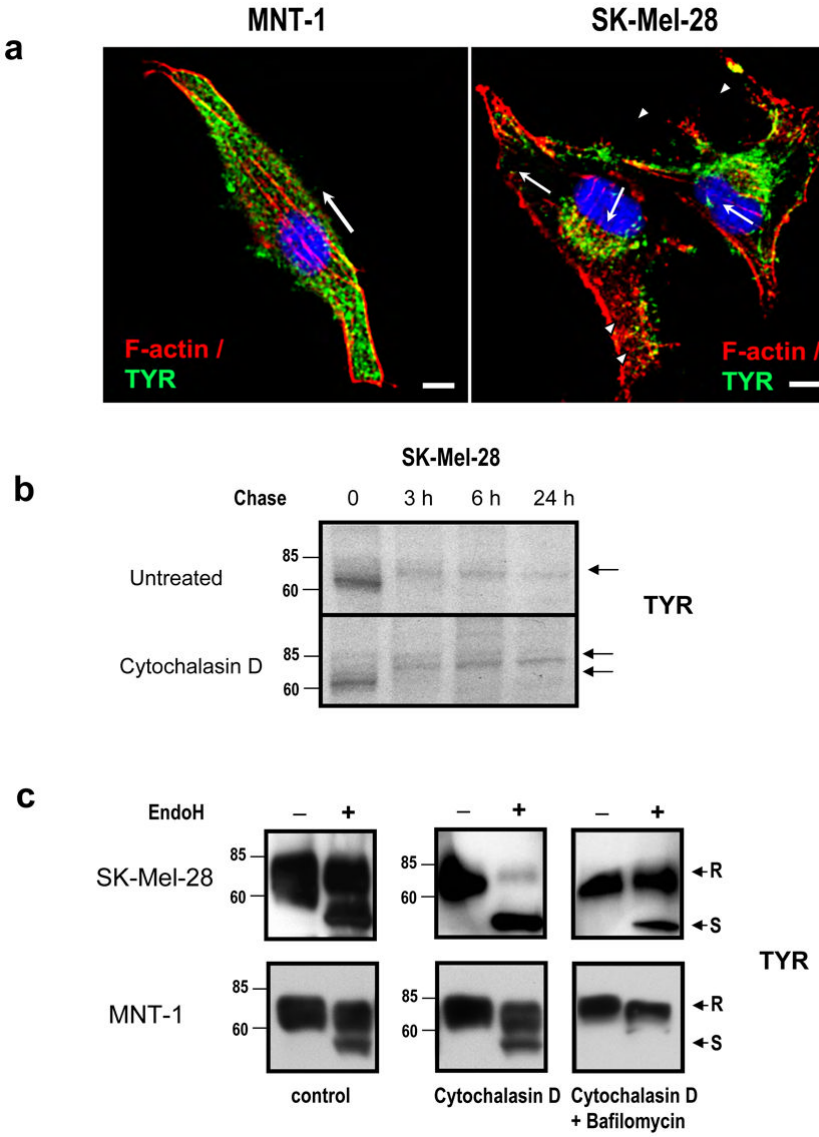

Figure 5. Effect of organellar pH on the trafficking of TYR

(A) Cells were fixed and stained with antibodies recognizing TYR (αPEP7h at 1:40; green) and actin filaments (phalloidin at 1:10; red). Nuclei were counterstained with DAPI (blue). Fluorescence images were collected by confocal microscopy. Scale bars = 10 μm **(B)** Cells were [^{35}S] metabolically labeled for 30 min and were treated with cytochalasin D. Immunoreactive bands were visualized by autoradiography. **(C)** Extracts were collected from cells treated or untreated with either cytochalasin D or cytochalasin D and bafilomycin for 3 hr before harvesting. Cell extracts were then digested with or without EndoH, and TYR was detected by Western blot. Bands resistant or sensitive to EndoH digestion are indicated as 'R' and 'S', respectively. Molecular weight markers are indicated on the left in kDa.

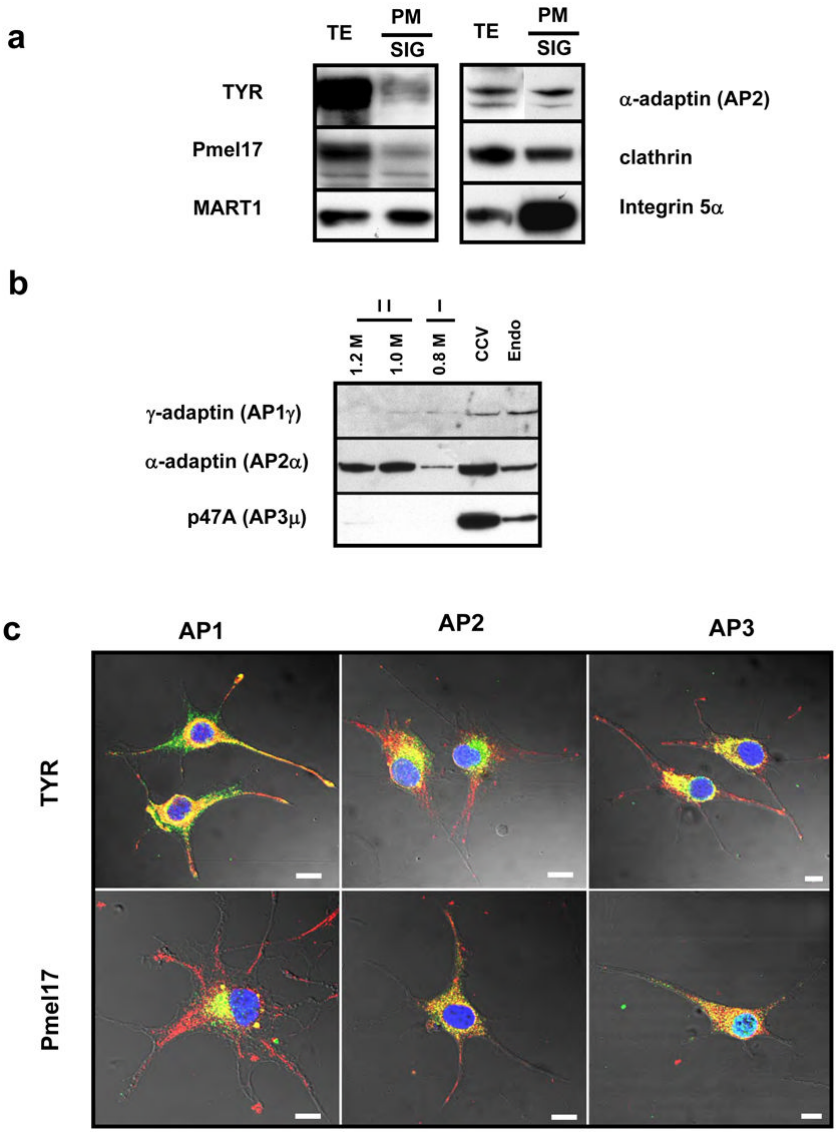

Figure 6. Localization of TYR and Pmel17 in SK-Mel-28 cells

(*A*) Plasma membrane proteins were recovered by SIG purification and were analyzed by immunoblotting. TYR, Pmel17 and MART-1 were detected in purified fractions. Integrin 4α was used as a positive control for plasma membrane proteins. Note the presence of AP2 and clathrin in the preparations. **(*B*)** Early melanosomes, clathrin coated vesicles and endosomes were isolated using sucrose gradients and were analyzed with antibodies against AP1γ, AP2α and AP3μ. Experiments were performed twice with comparable results. All samples were processed in parallel. **(C)** Cells were fixed and double stained for tyrosinase or Pmel17 (red) and AP1γ, AP2α or AP3μ (green) as indicated. Representative images for each combination are shown. Scale bars = 10 μm

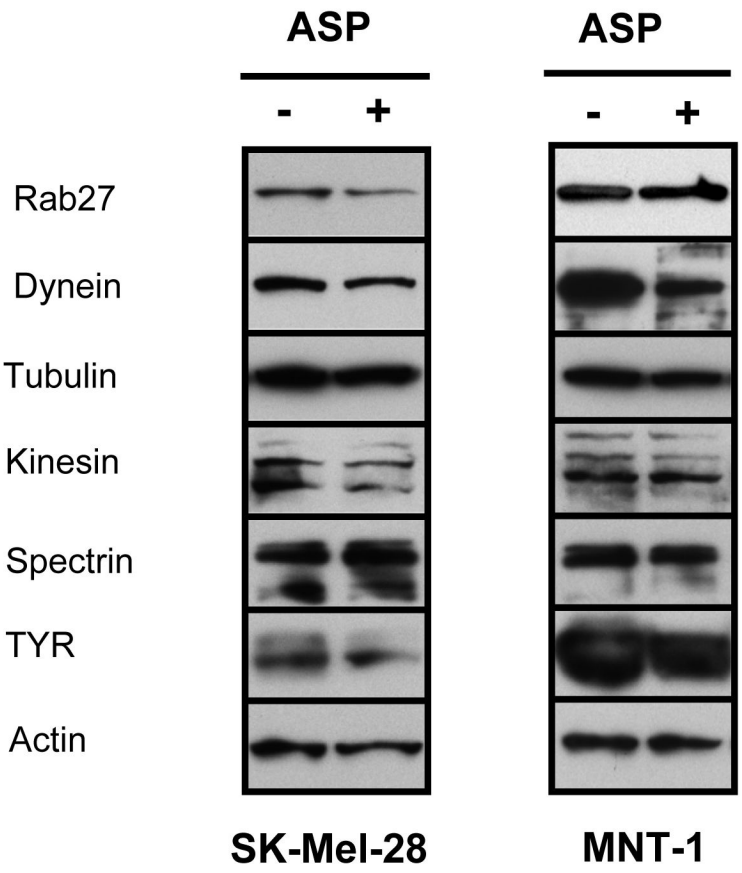

Figure 7.

Protein expression profile of motor proteins after ASP treatment of human melanoma cells. SK-Mel-28 cells (**A**) and MNT-1 cells (**B**) were treated for 3 days with or without ASP (1:500). New medium was added daily which contained either sterile water or ASP. Cell extracts were analyzed for protein levels of motor proteins and melanosomal proteins as noted. β-actin was used as a loading control. Images represent two different experiments.

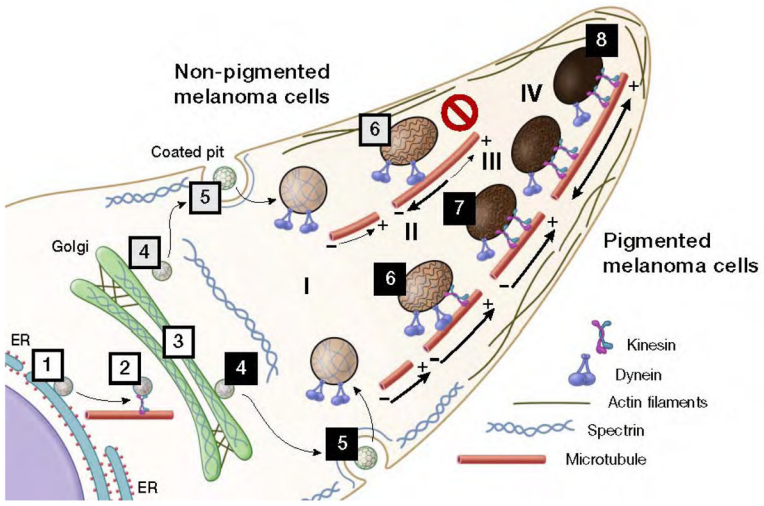

Figure 8. Scheme for the anterograde movement of sorting vesicles and transport of melanosomes in unpigmented (top) and in pigmented (bottom) melanoma cells

Vesicles containing melanosomal proteins bud from the ER (1). These vesicles are then moved forward by dynein/dynactin along microtubules to the *cis*-Golgi (2). In the Golgi, the spectrin mesh stabilizes the different arriving vesicles and continues the anterograde transport (3). Note, the presence of actin filaments at both ends of the Golgi cisternae providing support for this compartment and probably interacting with spectrin. At the TGN (4), sorting vesicles containing spectrin-like mosaics are delivered to downstream compartments in conjunction with other motor and budding systems (only delivery to the plasma membrane is shown to simplify the scheme). A new vesicle is then internalized (5) and directed to stage I melanosomes (6). The presence of dyneins in stage I and II melanosomes possibly favors its accumulation in the central area of the cell. Note that the spectrin-like mosaics in early melanosomes may help to stabilize the organelle and interact with either spectrin-adaptor proteins or some actin filaments (De Matteis and Morrow, 2000). In late melanosomes, the presence of kinesins promotes the transport of these organelles to the cell periphery using microtubules (7). Finally, stage IV melanosomes are transferred to actin filaments for secretion (8). Note, the major structural difference between unpigmented SK-Mel-28 cells (top) and pigmented MNT-1 cells (bottom) is the lack of spectrin in the plasma membrane.

Table 1

Motor-related proteins found in melanosomes by proteomics analysis

Protein AC/Gene ID	Protein	SK-Mel-28	MNT-1
P51159/RB27A	Rab-27	Stages I and II	all stages
Q9BV36/ MLPH	Melanophilin (SLAC2A)	N.D.	N.D.
Q9Y4I1/ MYO5A	Myosin-Va	N.D.	Stages II and IV
P33176/KINH	Kinesin heavy chain	N.D.	stage II
Q9H193	Kinesin 13A2	N.D.	stage IV
Q9NRC3/Q9NRC3	Cytoplasmic dynein heavy chain (Fragment)	Stage II	N.D.
Q14204/DYHC	Dynein heavy chain, cytosolic (DYHC)	Stages I and II	Stages II and IV
P63172/DYLT1	Dynein light chain Tctex-type 1	Stage 1	N.D.
P63167 DYL1	Dynein light chain 1, cytoplasmic	N.D.	Stages I and IV
Q9Y6G9/ DC1L1	Dynein 1 light intermediate chain	N.D.	Stage IV
Q14203/ DYNA	Dynactin-1	N.D.	Stage IV
Q13561/DCTN2	Dynactin subunit 2, Dynamitin	N.D.	Stage IV
Q9UQ16/DYN3	Dynamin 3	N.D.	Stage IV
Q13813/ SPTA2	Spectrin α chain, brain	Stages I and II	Stages II and IV
Q01082/ SPTB2	Spectrin β chain, brain 1	Stages I and II	Stages II and IV
Q9H254/ SPTN4	Spectrin β chain, brain 3	Stage II	N.D.
U49691/ANK1	Ankyrin	N.D.	N.D.
P58546/ MTPN	Myotrophin (protein V1)	Stage II	N.D.
P12814/ ACTN1	α-Actinin-1	Stages I and II	Stage IV
O43707/ ACTN4	α-Actinin-4 (F-actin cross linking protein)	Stages I and II	N.D.

Data taken from the melanosome proteome database, as reported by (Chi et al., 2006). N.D. = not detected

Table 2

Gene expression profiles of motor proteins after treatment of melan-a melanocytes with αMSH or ASP

Expression difference		Gene name
MSH	ASP	
ns	−1.9	RAB27A, member RAS oncogene family (Rab27a)
ns	−1.5	ARP1 actin-related protein 1 homolog B (yeast) (Actr1b)
1.5	−1.5	dynein, axonemal, intermediate polypeptide 2 (Dnai2)
ns	−1.9	dynein, axonemal, intermediate chain 1 (Dnaic1)
1.5	−1.5	tubulin, α4 (Tuba4)
ns	−1.6	tubulin-specific chaperone e (Tbce)
−1.6	ns	kinesin family member 15 (Kif15)
ns	−1.6	kinesin family member 21A (Kif21a)
ns	−1.5	kinesin family member 21B (Kif21b)

Statistically significant values ($p<0.01$ considering 6 analyses) are reported for genes differentially regulated by at least 1.5-fold, either by ASP or by αMSH, in melan-a melanocytes after 3 d of treatment. NS = not significant ($p>0.01$ or <1.5-fold).